Archives of Pharmacal Research (2023) 46:694–712
https://doi.org/10.1007/s12272-023-01460-3

Online ISSN 1976-3786
Print ISSN 0253-6269

Archives of Pharmacal Research
www.springer.com/12272

RESEARCH ARTICLE

Hyperoside attenuates pyrrolizidine alkaloids-induced liver injury by ameliorating TFEB-mediated mitochondrial dysfunction

Jie Xu[1,2,3] · Aizhen Xiong[1,3] · Xunjiang Wang[1,3] · Xing Yan[1,2,3] · Yilin Chen[1,2,3] · Xuanling Ye[1,3] · Zhengtao Wang[1,3] · Lili Ding[1,3] · Li Yang[1,2,3]

Received: 25 April 2023 / Accepted: 27 August 2023 / Published online: 21 September 2023

Abstract

Pyrrolizidine alkaloids (PAs) are potent hepatotoxins that can cause liver damage. Hyperoside (Hyp), a natural flavonoid, can be extracted from medicinal plants. Hyp displays hepatoprotective activity in various liver diseases. However, the potential effect and mechanism of action of Hyp in ameliorating PA-induced liver injury remain obscure. This study aimed to explore the protective effect of Hyp against PA-induced hepatotoxicity and its underlying mechanism. We established an in vitro model of PAs in mouse primary hepatocytes and developed a mouse model of acute PA toxicity to investigate the protective effect of Hyp. We found that Hyp notably attenuated PA-induced hepatotoxicity. RNA-sequencing showed that the beneficial effect of Hyp against PA-induced hepatotoxicity was associated with the transcription factor EB (TFEB)-peroxisome proliferator-activated receptor-γ coactivator-1-α (PGC1α) pathway. Our results confirmed that both the autophagy-lysosomal pathway and mitochondrial biogenesis were induced by Hyp through TFEB nuclear translocation in PA-induced liver injury. Furthermore, we demonstrated that activation of the mechanistic target of rapamycin complex 1 (mTORC1) by MHY 1485 decreased TFEB nuclear translocation and abrogated the protective effect of Hyp against PA-induced liver injury in mice. In contrast, inhibition of mTORC1 activity increased the level of TFEB and reduced hepatotoxicity induced by PAs in mouse livers. Likewise, Hyp-induced TFEB activation was validated in vitro. In conclusion, Hyp can activate the TFEB-mediated autophagy-lysosomal pathway and mitochondrial biogenesis through inhibition of mTORC1 activity, alleviating the liver injury induced by PAs, thus suggesting the potential value of Hyp in the treatment of PA-induced hepatotoxicity.

Keywords Hyperoside · Pyrrolizidine alkaloids · Transcription factor EB · Mitochondrial dysfunction · Liver injury

Introduction

Drug-induced liver injury (DILI) or drug-induced hepatotoxicity commonly refers to any kind of hepatic injury caused by prescription medications, dietary/herbal supplements, or xenobiotics (Kaplowitz 2005; Navarro and Senior 2006; Chalasani et al. 2021). Chronic application or overdosing of anti-infectious, anti-tuberculosis, and natural pharmaceuticals is the most common cause of DILI (Leise et al. 2014). According to a survey, the incidence rate of DILI is higher in China than in Western countries. Interestingly, the uncontrolled use of traditional Chinese medicines (TCMs) or herbal products is considered the major cause of the increased rate of DILI in China (Shen et al. 2019). Hepatic sinusoidal obstruction syndrome (HSOS) is a hepatic vascular disease that typically manifests with tender hepatomegaly, ascites, and hyperbilirubinemia (Wang and Gao 2014). In the absence of medical treatment, HSOS can

✉ Lili Ding
nail8219@126.com

✉ Li Yang
yangli7951@hotmail.com

1 Shanghai Key Laboratory of Complex Prescriptions, The MOE Key Laboratory for Standardization of Chinese Medicines and the SATCM Key Laboratory for New Resources and Quality Evaluation of Chinese Medicines, Institute of Traditional Chinese Materia Medica, Shanghai University of Traditional Chinese Medicine, Cai Lun Road 1200, Zhangjiang, Shanghai 201203, China

2 Institute of Interdisciplinary Integrative Medicine Research, Shanghai University of Traditional Chinese Medicines, Shanghai 201203, China

3 Shanghai R & D Center for Standardization of Traditional Chinese Medicines, Shanghai 201203, China

lead to severe consequences, including fibrosis, cirrhosis, necrosis, and eventually death (Wang et al. 2018). The main cause of HSOS in China is ingestion of the Chinese herb *Gynura japonica* (Thunb.) Juel (*G. japonica*), which produces pyrrolizidine alkaloids (PAs). Unintentional consumption of this herb causes 50%–89% of reported HSOS cases. It has been indicated that more than 8000 cases of chronic liver injury could be due to intake of naturally sourced PAs in high amounts (Stegelmeier et al. 1999; Wang and Gao 2014). Thus, PAs are potent hepatotoxins, and there is an urgent need to develop new preventive and therapeutic strategies to ameliorate PA-induced liver dysfunction.

DILI shares common characteristics of mitochondrial dysfunction. Increasing numbers of studies have demonstrated that PA-induced hepatotoxicity involves mitochondrial damage in liver cells (Lu et al. 2018; Zheng et al. 2021). Mitochondria are important cellular energy sources, involved in many crucial cellular processes, including the production of energy molecules such as adenosine triphosphate (ATP) through oxidative phosphorylation (OXPHOS), generation and detoxification of reactive oxygen species (ROS), regulation of cellular calcium homeostasis, substrate metabolism, and apoptosis (Liesa et al. 2009; Murphy 2009; Hunt 2010). Mitochondrial stress or damage signaling stimulates mitochondrial biogenesis to replace injured mitochondria (Han et al. 2013). Physiologically, mitochondrial biogenesis regulates the total mitochondrial mass per cell to maintain energy homeostasis during energy deprivation or following mitochondrial damage (Mansouri et al. 2018). Transcription Factor EB (TFEB) acts as the major regulator of mitochondrial biogenesis (Settembre et al. 2013; Ma et al. 2015). TFEB-mediated mitochondrial quality control is an important endogenous regulatory mechanism of mitochondrial homeostasis. Therefore, TFEB could be a potential target for the treatment of PA-induced mitochondrial dysfunction.

TFEB, a crucial member of the microphthalmia family (MiT/TFE) of proteins, is also a master regulator of autophagy-related gene transcription (Settembre et al. 2011). Autophagy is a highly conserved cellular process that removes dysfunctional organelles, misfolded proteins, and damaged mitochondria via the lysosomal degradation pathway, after which the degraded biomolecular components are recycled through complex biosynthetic pathways (Nakatogawa et al. 2009; Mizushima and Komatsu 2011). Lysosomal catabolites are transported from lysosomes by certain export proteins to different types of cell and organelle membranes for diverse biological functions (Ruivo et al. 2009; Settembre et al. 2013). Activated TFEB regulates the activation of a subset of autophagy-related genes, thereby modulating lysosome biogenesis and activity (Roczniak-Ferguson et al. 2012; Martina et al. 2012; Settembre et al. 2013). From this perspective, targeting the TFEB-mediated autophagy-lysosomal pathway may ameliorate PA-induced liver injury.

Hyperoside (Hyp), a flavonol glycoside compound, can be extracted from medicinal herbs (Middleton et al. 2000). Many studies have suggested that Hyp has extensive pharmacological properties, including hepatoprotective, anti-inflammatory, antithrombotic, antioxidative, antifungal, and anticancer properties (Raza et al. 2017; Zhu et al. 2017). In addition, studies have demonstrated the hepatoprotective effects of Hyp under a series of disease conditions, such as acetaminophen (APAP)-induced liver damage, carbon tetrachloride-induced hepatotoxicity, and cisplatin-induced liver injury (Xie et al. 2016; Niu et al. 2017; Xing et al. 2020). Therefore, we hypothesized that Hyp might be an effective drug to treat PA-induced hepatotoxicity.

In this study, we examined the effectiveness of Hyp in alleviating mitochondrial dysfunction in PA-induced liver injury and explored the underlying mechanism of action of this natural product. Our experimental results illustrated that Hyp-activated TFEB-mediated autophagy-lysosomal pathway and mitochondrial biogenesis through inhibition of the mechanistic target of rapamycin complex 1 (mTORC1) activity rescued liver cells from PA toxicity. The outcomes of this investigation provide essential data for the subsequent clinical development of Hyp as an innovative drug for the treatment and/or prevention of HSOS.

Materials and methods

Reagents

Total alkaloid extract (TA) isolated from *G. japonica* was purchased from Chengdu Biopurify Phytochemicals Ltd. (Chengdu, China). TA was analyzed by UPLC-diode-array detection-mass spectrometry (MS). The content of PAs in TA was determined according to a previously described method to ensure proper extraction of active ingredients (Xiong et al. 2019). First, TA was dissolved in 5% HCl, and then the pH was adjusted to 6–7 by adding 5 mM NaOH. Finally, the working concentration of TA was attained via the addition of saline to the TA solution. Purified Hyp was purchased from Shanghai Standard Technology Co. Ltd. (Shanghai, China).

Animal experiments

C57BL/6J mice (8 weeks old) were purchased from the Laboratory Animal Center of Shanghai University of Traditional Chinese Medicine (SHUTCM, Shanghai, China). The experimental animals were housed in a specific pathogen-free (SPF) environment with a standard laboratory diet and free access to tap water. All animal studies have been

approved by the Shanghai University of Traditional Chinese Medicine Experimental Animal Ethical Committee.

In the first set of experiments, mice were randomly divided into five groups with six mice per group: the (1) vehicle, (2) TA, (3) TA + Hyp (20 mg/kg), (4) TA + Hyp (40 mg/kg), and (5) TA + Hyp (80 mg/kg) groups. The mice were orally (*p.o.*) administered 100 mg/kg TA or vehicle once and then subjected to two administrations of different doses of Hyp (20, 40, and 80 mg/kg, *p.o.*) at 6 h and 30 h post-TA treatment. The mice were sacrificed at 48 h after TA administration, and the blood and liver samples were harvested immediately.

In the second set of experiments, mice were similarly divided into five groups with six mice per group: the (1) vehicle, (2) TA, (3) TA + Hyp, (4) TA + Hyp + chloroquine (CQ), and (5) CQ groups. CQ (HY-17589A) was purchased from MedChemExpress (Shanghai, China). The mice were *p.o.* administered 100 mg/kg TA or vehicle once, and then subjected to two Hyp treatments (40 mg/kg, *p.o.*) at 6 h and 30 h post-TA administration. CQ (40 mg/kg) was intraperitoneally (*i.p.*) injected into mice 1 h before Hyp administration. The mice were sacrificed at 48 h after TA administration, and their blood and liver samples were collected accordingly.

In the third set of experiments, mice were similarly divided into six groups with five mice per group. We set six groups to receive tail vein injection of small interfering RNA (siRNA) against TFEB or negative control (NC) (provided by RiboBio, Guangzhou, China) before TA administration. The mice were *p.o.* administered 100 mg/kg TA or vehicle once, and then subjected to two Hyp treatments (40 mg/kg, *p.o.*) at 6 h and 30 h post-TA administration. The mice were sacrificed at 48 h after TA administration, and the blood and liver samples were harvested immediately.

In the fourth set of experiments, mice were similarly divided into seven groups with six mice per group: the (1) vehicle, (2) TA, (3) TA + Hyp, (4) TA + Hyp + MHY 1485, (5) TA + Torin1, (6) MHY 1485 (HY-B0795, MedChemExpress, Shanghai, China), and (7) Torin1 (HY-13003, MedChemExpress, Shanghai, China) groups. The mice were *p.o.* administered 100 mg/kg TA or vehicle once and then subjected to two administrations of Hyp (40 mg/kg, *p.o.*) at 6 h and 30 h post-TA administration. MHY 1485 (10 mg/kg) or torin1 (1 mg/kg) was *i.p.* injected into mice at 1 h before Hyp administration or at 6 h post-TA administration, respectively. The mice were sacrificed at 48 h after TA administration, and the blood and liver samples were collected immediately.

Serum biochemistry analysis

To detect serum levels of alanine aminotransferase (ALT), aspartate aminotransferase (AST), and total bile acid (TBA), serum samples were prepared from fresh blood. The ALT, AST, and TBA levels were measured using an Enzymatic Assay Kit (Nanjing Jiancheng Bioengineering Institute, Nanjing, China), according to the manufacturer's protocol.

Histopathological analysis

After fixing liver tissue samples in 4% paraformaldehyde (PFA) and embedding them in paraffin, the tissue sections were cut into 5 μm slices, stained with hematoxylin–eosin (H&E), and observed under a light microscope (Olympus Corp., Tokyo, Japan). For immunofluorescence (IF) staining, liver paraffin sections were blocked with 5% serum in phosphate-buffered saline (PBS) and then probed with anti-TFEB antibody (1:100, 13372-1-AP, Proteintech Group, Rosemont, PA, USA). After being washed, the sections were stained with horseradish peroxide (HRP)-conjugated secondary antibody and the nuclei were counterstained with DAPI (C1006, Beyotime Biotechnology, Shanghai, China). Images were acquired with a fluorescence microscope.

Transmission electron microscopy (TEM)

Freshly harvested liver tissues were fixed in 2.5% glutaraldehyde, dehydrated in a graded ethanol series, and embedded in Epon. After cutting the embedded tissues into ultrathin slices, the sections were stained with uranyl acetate followed by lead citrate and finally examined under a TEM.

Primary hepatocyte culture and treatment

Mouse primary hepatocytes were isolated from male C57BL/6J mice (7–8 weeks old) using the collagenase type IV perfusion technique (Yang et al. 2017). All primary hepatocytes were incubated in William's E medium containing 10% fetal bovine serum (FBS), 1% penicillin–streptomycin, and 1% L-glutamine (Gibco, Carlsbad, CA, USA) in a humidified incubator at 37 ℃ with 5% CO_2.

For in vitro experiments, primary hepatocytes were cultured overnight in a serum-containing medium. Hyp (5, 10, 25, 50, 100 μM) pretreatments were initiated 1 h before and continuing through TA (1.34 mg/mL) treatment for 12 h or 24 h. To evaluate the effect of mTORC1 inhibition or activation on hepatoprotection by Hyp in a PA-induced liver injury model, primary hepatocytes were pretreated with Torin1 (500 nM) for 1 h and then treated with TA for 12 h or 24 h. MHY 1485 (500 nM) was added to the primary hepatocyte culture 1 h before initiating Hyp (50 μM) treatment, and the

cells were then continuously treated with TA for 12 h or 24 h after the end of 1 h of Hyp treatment.

Adenoviruses and siRNA transfection

Mouse primary hepatocytes were transfected with adenoviruses harboring mRFP-GFP-LC3 (Hanbio Biotechnology, Shanghai, China). After treating these virus-infected cells with TA and/or Hyp, yellow and red puncta were observed using a cell imaging multimode reader (BioTek Cytation5, Agilent, Palo Alto, CA, USA). Mouse primary hepatocytes were transfected with siRNA against TFEB or scramble siRNA (scRNA) using a FECT™ CP Transfection Kit (RiboBio, Guangzhou, China). The siRNA sequences used were as follows: sense 5′-GACTCAGAAGCGAGAGCT ATT-3′ and antisense 5′-UAGCUCUCGCUUCUGAGU CTT-3′. After TA and Hyp treatments, siRNA-transfected cells were assayed by immunoblotting (IB).

Lysosomal staining

Lysosomes in primary hepatocytes were labeled with LysoTracker and LysoSensor. LysoTracker was used to detect lysosome abundance, and LysoSensor was used to detect changes in lysosomal pH. Treated primary hepatocytes were incubated with 75 nM LysoTracker Red DND-99 (L7528, Thermo Fisher Scientific) or 1 μM LysoSensor Green DND-189 (L7535, Thermo Fisher Scientific, Waltham, MA, USA) at 37 °C for 30 min. IF images were captured using a cell imaging multimode reader, and the fluorescence intensities in the respective treatment groups were analyzed using a multimode reader (SPARK 10M, TECAN, Switzerland).

IF analysis

For IF staining in vitro, primary hepatocytes were fixed with 4% PFA for 20 min, permeabilized with 0.5% Triton X-100 for 20 min, and blocked in 2% BSA for 2 h. Then, the hepatocytes were immunolabeled with primary antibodies anti-TFEB (1:100, 13372-1-AP, Proteintech Group, Rosemont, PA, USA), anti-LAMP1 (1:100, ab208943, Abcam, Boston, MA, USA), and anti-LAMP2 (1:100, NB300-591, Novus Biologicals, Littleton, CO, USA) overnight at 4 °C. The next day, the hepatocytes were stained with Alexa Fluor 647-conjugated secondary antibodies (4414 or 4410, Cell Signaling Technology, Boston, MA, USA) for 1 h, and the nuclei were counterstained with DAPI for 5 min at room temperature. IF images were visualized using a cell imaging multimode reader.

Quantitative real-time PCR (qRT-PCR) analysis

Total RNA from liver tissues or primary hepatocytes was isolated using an RNA Purification Kit (EZB-RN001-plus or B0004DP, EZBioscience, Roseville, CA, USA), and cDNA was synthesized using Evo M-MLV RT Premix (AG11706, Accurate Biology, Hunan, China) reagent, according to the manufacturer's instructions. The qRT-PCR assay was performed using a SYBR® Green qPCR Kit (AG11718, Accurate Biology, Hunan, China) in a real-time PCR detector. The relative expression of target genes was normalized to that of GAPDH and evaluated using the $2^{-\Delta\Delta Ct}$ method and is reported as the ratio to vehicle. Table 1 contains an inventory of the primer sequences.

RNA-sequencing analysis

Total RNA was isolated from fresh liver tissues using the TRIzol method according to the manufacturer's protocol. Total amounts and integrity of RNA were assessed using a RNA Nano 6000 Assay Kit on a Bioanalyzer 2100 system (Agilent, Palo Alto, CA, USA). Total RNA was used as input material for the RNA sample preparations. Briefly, mRNA was purified through the use of poly-T oligo-attached magnetic beads, fragmented, and reverse-transcribed. The cDNA was end-repaired, and a single 'A' base was added. Adaptor ligation, purification, and enrichment using PCR were performed. The fragments of the library were purified using the AMPure XP system

Table 1 Primer sequences for qRT-PCR

Primer	Sequence (5'-3')
Map1lc3b	F: AGCAATGGCTGTGTAAGACTC R: CGCTGGTAACATCCCTTTTT
Uvrag	F: GGCTGAATGATGGCTACTACG R: AACACAGTTCTGGTCCACCTG
Wipi1	F: CTGTCATCCGAGTGTTCTCTG R: GGAACTGGGAGTCCATACTGA
Lamp1	F: TAAGAAGCAAACGGGAGCAGG R: CCAAGCCAAGTGTCCAGAGGT
Pgc1α	F: ATCTGGGTGGGAGAGGATACT R: TAGGTGTCAGGACAAAGGACA
Cpt1α	F: AGCTCGCACATTACAAGGACA R: CCAGCACAAAGTTGCAGGAC
Pparα	F: GAGGATGGGGACTTTTGTTCT R: GGCTTTTTGGCTGTAGGAGG
Nrf1	F: TACTCTGCTGTGGCTGATGGA R: ATGCTTGCGTCGTCTGGAT
Tfam	F: CGGAGACATCTCTGAGCATTA R: AAGGCTTTGAGACCTAACTGG
Gapdh	F: AAATGGTGAAGGTCGGTGTG R: AGGTCAATGAAGGGGTCGTT

(Beckman Coulter, Brea, CA, USA), and the Agilent 2100 Bioanalyzer was used for the quality control analysis. High-quality libraries were then sequenced on an Illumina NovaSeq 6000 platform.

Isolation of nuclear and cytoplasmic protein fractions and western blotting (WB)

Nuclear and cytoplasmic extracts were prepared using a Nuclear and Cytoplasmic Protein Extraction Kit (20126ES60, Yeasen Biotechnology, Shanghai, China), according to the manufacturer's protocol. For the WB assay, liver tissue or primary hepatocytes were extracted using RIPA buffer (89900, Thermo Fisher Scientific, Waltham, MA, USA) containing protease inhibitor cocktail (539134, Merck Millipore, Darmstadt, Germany), as described elsewhere (Yang et al. 2017). Protein expression was quantified using densitometric analyses (ImageJ software). The relative fold differences in expression levels were standardized to the GAPDH or Histone H3 levels. The following primary antibodies were used: anti-phospho-mTOR (Ser2448) (5536), anti-mTOR (2983), anti-phospho-p44/42 MAPK (ERK1/2) (Thr202/Tyr204) (4370), anti-p44/42 MAPK (ERK1/2) (137F5) (4695), anti-phospho-S6 (Ser235/236) (4858), anti-S6 (2217), anti-TFEB (32361), anti-cytochrome C (11940), anti-CPT1α (12252), anti-GAPDH (5174), anti-Histone H3 (4499), and anti-α-tubulin (3873) (all from Cell Signaling Technology, Boston, MA, USA); anti-SQSTM1/p62 (ab109012), anti-LC3B (ab192890), anti-Lamp1 (ab208943), anti-PGC1α (ab54481), anti-COX IV (ab202554), anti-phospho-eIF4E (ab76256), and anti-eIF4E (ab33766) (all from Abcam, Boston, MA, USA); and anti-PPARα (NB300-537, from Novus Biologicals). An HRP-conjugated AffiniPure goat anti-rabbit IgG (H+L) (SA00001-2) secondary antibody was purchased from Proteintech Group (Rosemont, PA, USA).

ATP level measurement

The levels of intracellular ATP (ab113849, Abcam, Boston, MA, USA) and serum ATP (abs580117, Absin, Shanghai, China) were examined using an ATP Assay Kit according to the manufacturer's instructions. Briefly, cell or serum samples were lysed with lysis buffer in 96-well black-walled plates, after which ATP detection reagent was added to each well. A multimode reader was successfully used to detect luminescence.

Mitochondrial mass and mitochondrial membrane potential (Δψm) assessment

To evaluate changes in mitochondrial mass, primary hepatocytes were incubated with MitoTracker Green (M7514, Thermo Fisher Scientific, Waltham, MA, USA) at 37 °C for 30 min to visualize mitochondrial morphology. Images were captured by a cell imaging multimode reader. The Δψm was measured with JC-1 dye using a JC-1-based Mitochondrial Membrane Potential Assay Kit (C2006, Beyotime Biotechnology, Shanghai, China). The fluorescence intensity of JC-1 was examined by a multifunctional microplate reader.

Mitochondria isolation

Mitochondria were isolated from liver tissues or primary hepatocytes using a Mitochondrial Isolation Kit (89801 or 89874, Thermo Fisher Scientific, Waltham, MA, USA) according to the manufacturer's instructions. The extracted cytosolic and mitochondrial fractions were assayed by IB.

Statistical analysis

The experimental results are expressed as the mean ± SD or SEM. GraphPad Prism 8 (GraphPad Software, San Diego, CA, USA) was used for data analysis. Comparisons between the two groups were carried out using Student's *t*-test, and comparisons among three or more groups were performed using one-way analysis of variance (ANOVA). The results were determined to be statistically significant for P values of < 0.05.

Results

Hyp attenuates PA-induced liver injury in vivo

To explore the beneficial effect of Hyp on PA-induced liver injury, male C57BL/6J mice were administered TA (100 mg/kg, *p.o.*) and were then administered Hyp (20, 40, or 80 mg/kg, *p.o.*) twice at 6 h and 30 h post-TA administration (Fig. 1A). As shown in Fig. 1B–D, serum biochemical analysis revealed that Hyp reduced the levels of ALT, AST, and TBA in the TA-treated mice. H&E staining further showed that TA induced severe liver damage, including necrosis of hepatocytes, intrahepatic hemorrhage, and detachment of hepatic sinusoidal endothelial cells. Interestingly, a higher dose of Hyp (40, 80 mg/kg) reversed all these adverse events, while mild changes were observed in mice treated with a low dose of Hyp (20 mg/kg) (Fig. 1E). Collectively, these results suggest that Hyp may alleviate PA-induced hepatotoxicity in vivo. Since 40 mg/kg and 80 mg/kg Hyp showed similar effects on PA-induced hepatotoxicity recovery, we used 40 mg/kg Hyp for all subsequent animal experiments.

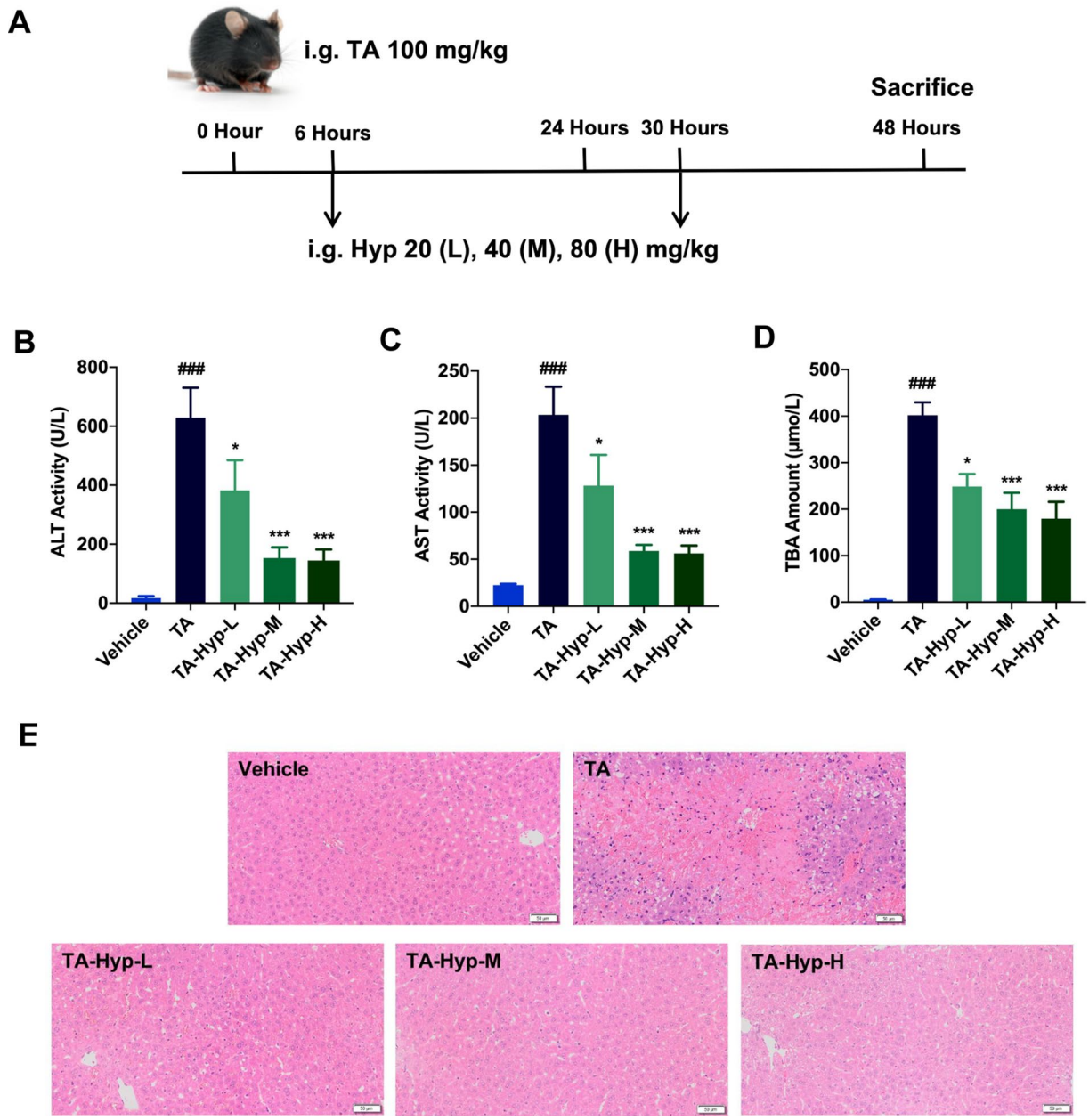

Fig. 1 Hyp attenuates PA-induced liver injury in mice. **A** The mice were orally administered TA and then subjected to two administrations of Hyp at 6 h and 30 h post-TA treatment. The mice were sacrificed at 48 h after TA administration. **B** Serum ALT activity. **C** Serum AST activity. **D** Serum TBA amount. **E** Representative images of H&E-stained liver sections (scale bars, 50 μm). Data were shown as the means ± SEM (n = 6) and analyzed by one-way ANOVA. $^{###}P < 0.001$ vs. Vehicle; $^{*}P < 0.05$, $^{***}P < 0.001$ vs. TA

Hyp improves mitochondrial function in a PA-induced liver injury mouse model

Transcriptomic analysis was performed on liver tissues obtained from the vehicle, TA, and TA-Hyp-M mice to examine the beneficial effects of Hyp on PA-induced liver injury at the molecular level. We found that TA led to a substantial difference in gene expression profiles between the TA-treated and vehicle-treated animal groups. Compared with TA treatment alone, TA-Hyp-M treatment upregulated 147 genes and downregulated 261 genes (Fig. 2A). Gene Ontology (GO) analysis of relevant biological process (BP) pathways revealed that the genes affected by Hyp treatment were related to mitochondrial organization (Fig. 2B). These results suggest an important role of Hyp in regulating mitochondrial homeostasis in PA-induced liver injury. Next, we investigated whether Hyp attenuated mitochondrial dysfunction in PA-treated mice. TEM analysis revealed that

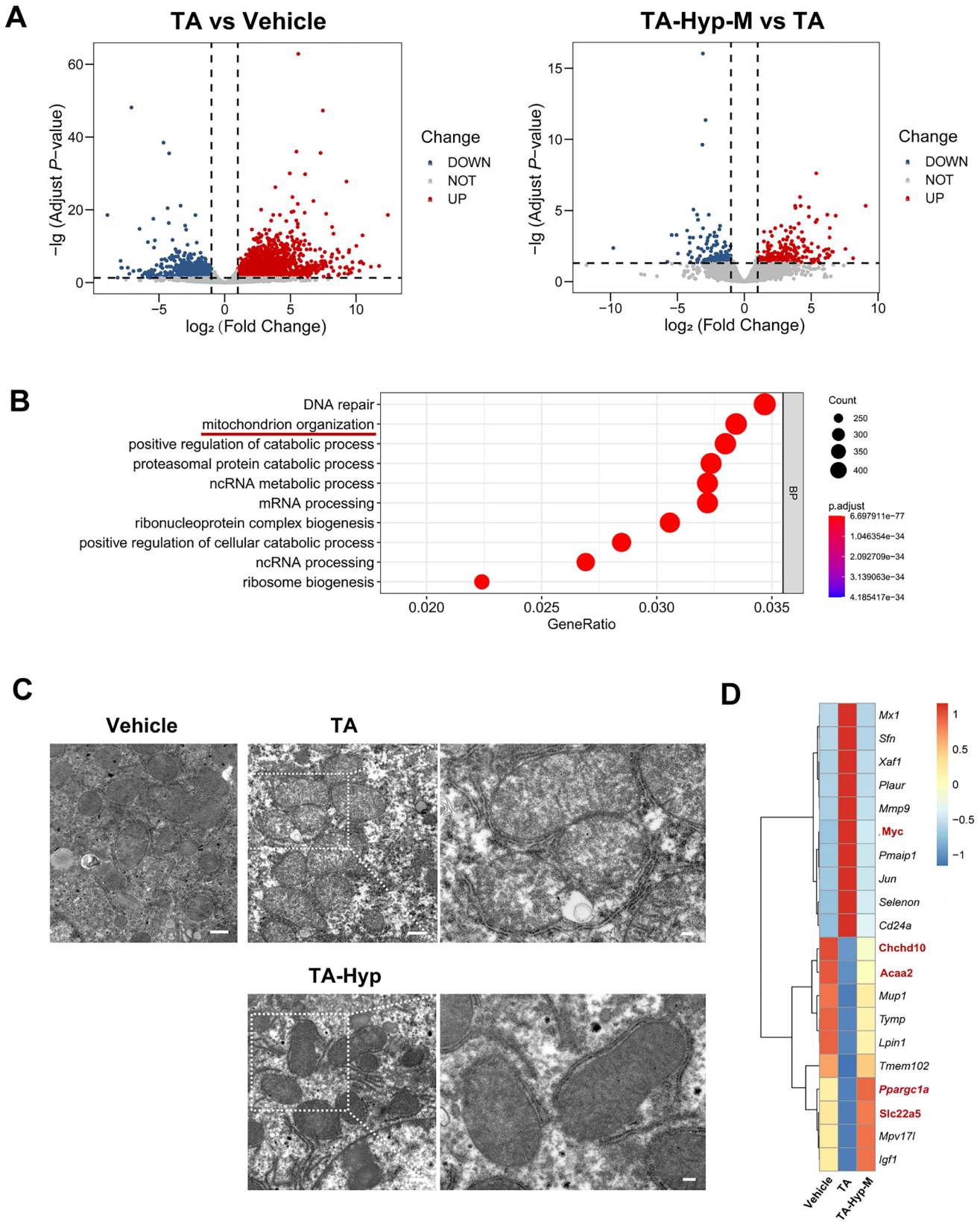

Fig. 2 Hyp attenuates mitochondrial dysfunction in PA-induced liver injury. **A** RNA-sequencing analysis of the mouse liver: volcano plot illustrating upregulated (red) and downregulated (blue) genes, TA compared Vehicle, TA-Hyp-M compared TA. **B** GO analysis of BP in TA, TA-Hyp-M mouse liver. **C** Representative TEM micrographs of mouse liver mitochondria from each group. Scale bars, 2 μm (wireframe indicates the magnified image). **D** Heatmap showing the top 20 expression profiles of genes related to mitochondrion organization in different groups

TA-treated mice had mitochondrial abnormalities, including disorganized cristae, vacuolation, and a smaller and rounded mitochondrial appearance. However, the addition of Hyp resulted in a remarkable reversal of PA toxicity, as observed by relatively healthy and unfragmented mitochondria (Fig. 2C). The top 20 differentially expressed genes (DEGs), including 10 downregulated and 10 upregulated genes, are listed and clustered in Fig. 2D. The upregulated genes *Chchd10*, *Acaa2*, *Pgc1α* and *Slc22a5* and the downregulated gene *Myc* were found to be regulated by TFEB. We paid particular attention to peroxisome proliferator-activated receptor-γ coactivator-1-α (PGC1α), which is a central regulator of mitochondrial biogenesis and plays a key role in energy balance and metabolism. Moreover, PGC1α activity is directly regulated by TFEB (Ma et al. 2015). TFEB-mediated mitochondrial quality control is an important endogenous signaling regulatory mechanism in maintaining mitochondrial homeostasis. Given the positive effects of TFEB on regulating mitochondrial function, these results suggest that TFEB may be involved in mediating the beneficial effects of Hyp treatment on PA-induced liver injury.

Hyp attenuates PA-induced liver injury by enhancing autophagy

TFEB mainly regulates autophagy-lysosomal pathway-associated gene expression (Sardiello et al. 2009; Settembre et al. 2011). To explore whether Hyp was able to alleviate liver injury in TA-treated mice through autophagy activation, we performed TEM. A few autophagosome-like vesicles were observed in the livers of TA-treated mice. In contrast, many autophagosome-like vesicles were observed in the liver sections from Hyp-treated mice (Fig. 3A). Autophagy initiation is followed by the lipidation of cytosolic LC3-I forming LC3-II (an autophagy indicator), which then binds to the autophagosome membrane and undergoes degradation in lysosomes as a portion of autophagic cargo (Qian et al. 2021). SQSTM1/p62 (an autophagy-selective substrate) is widely used as a predictor of autophagic flux. The abundance of autophagy substrates increases when the autophagic degradation system is impaired. WB analysis demonstrated a lower LC3-II level in the TA group of mice concomitant with a higher level of SQSTM1/p62, indicating blockade of the autophagy-lysosomal degradation pathway. Hyp reversed the inhibition of autophagy in TA mice by increasing the expression of LC3-II while decreasing the expression of SQSTM1/p62 (Fig. 3B). Moreover, TA significantly decreased the mRNA levels of autophagy-associated hepatic *Map1lc3b*, *Uvrag* and *Wipi1* genes in comparison to those in vehicle-treated mice. Hyp treatment effectively reversed these reductions (Fig. 3C). As shown in Supplementary Fig. 1A, we also noticed that Hyp reversed the reduction in LC3-II expression and increased SQSTM1/p62 accumulation in primary hepatocytes. To further confirm the role of Hyp in autophagy activation, we administered CQ (an autophagy inhibitor) to TA-treated mice. We found that CQ exacerbated the Hyp-induced decreases in the activity of serum ALT and AST as well as the level of TBA (Fig. 3D–F). H&E staining also illustrated that CQ induced severe liver damage, including hepatocellular necrosis and intrahepatic hemorrhage (Fig. 3G). CQ further reversed the mRNA levels of autophagy-associated genes after Hyp treatment in TA-treated mice (Fig. 3H). These data suggest that PAs can impair the autophagy pathway, while Hyp may attenuate liver injury by activating autophagy.

To further investigate the potential mechanism of the Hyp-mediated alleviation of PA-induced liver injury through autophagic flux activation, primary hepatocytes were treated with Hyp in the absence or presence of bafilomycin A1 (Baf A1), a lysosomal degradation inhibitor. We found that Hyp exposure increased the formation of LC3-II after treatment with Baf A1 (Supplementary Fig. 1B), suggesting that Hyp activates hepatic autophagic flux. Additionally, primary hepatocytes were infected with mRFP-GFP-LC3 adenoviruses to determine whether Hyp can stimulate autophagic flux. Analysis of GFP fluorescence intensity revealed that LC3 overexpression readily suppressed the acidity of autolysosomes. Nevertheless, since mRFP is more stable in an acidic medium, it was easy to locate both autophagosomes and autolysosomes labeled with RFP. By using this method, we discovered that TA-activated primary hepatocytes had a much greater proportion of GFP signals, indicating the accumulation of nonacidic autophagosomes. Hyp increased the amount of mRFP signals in primary hepatocytes (Supplementary Fig. 1C). These results demonstrated that autophagy might be enhanced without blockade of the fusion of autophagosomes and lysosomes. Together, our results strongly suggest that Hyp can alleviate PA-induced liver injury by enhancing autophagic flux.

Hyp attenuates PA-induced impairment of lysosomal function

Lysosomes are terminal degradative organelles that ensure the completion of autophagic flux. Hence, we investigated how Hyp might impact the induction of lysosomal function in primary hepatocytes during PA exposure. The abundance and acidification of lysosomes were determined using LysoTracker Red and the pH-sensitive LysoSensor Green, respectively. The number of lysosomes was drastically reduced in primary hepatocytes after TA treatment. This was indicated by a reduction in the number of red puncta in LysoTracker staining. Additionally, after TA treatment, the LysoSensor Green fluorescence signal intensity was decreased in primary hepatocytes, indicative of defective lysosomal acidification, and this reduction was reversed by

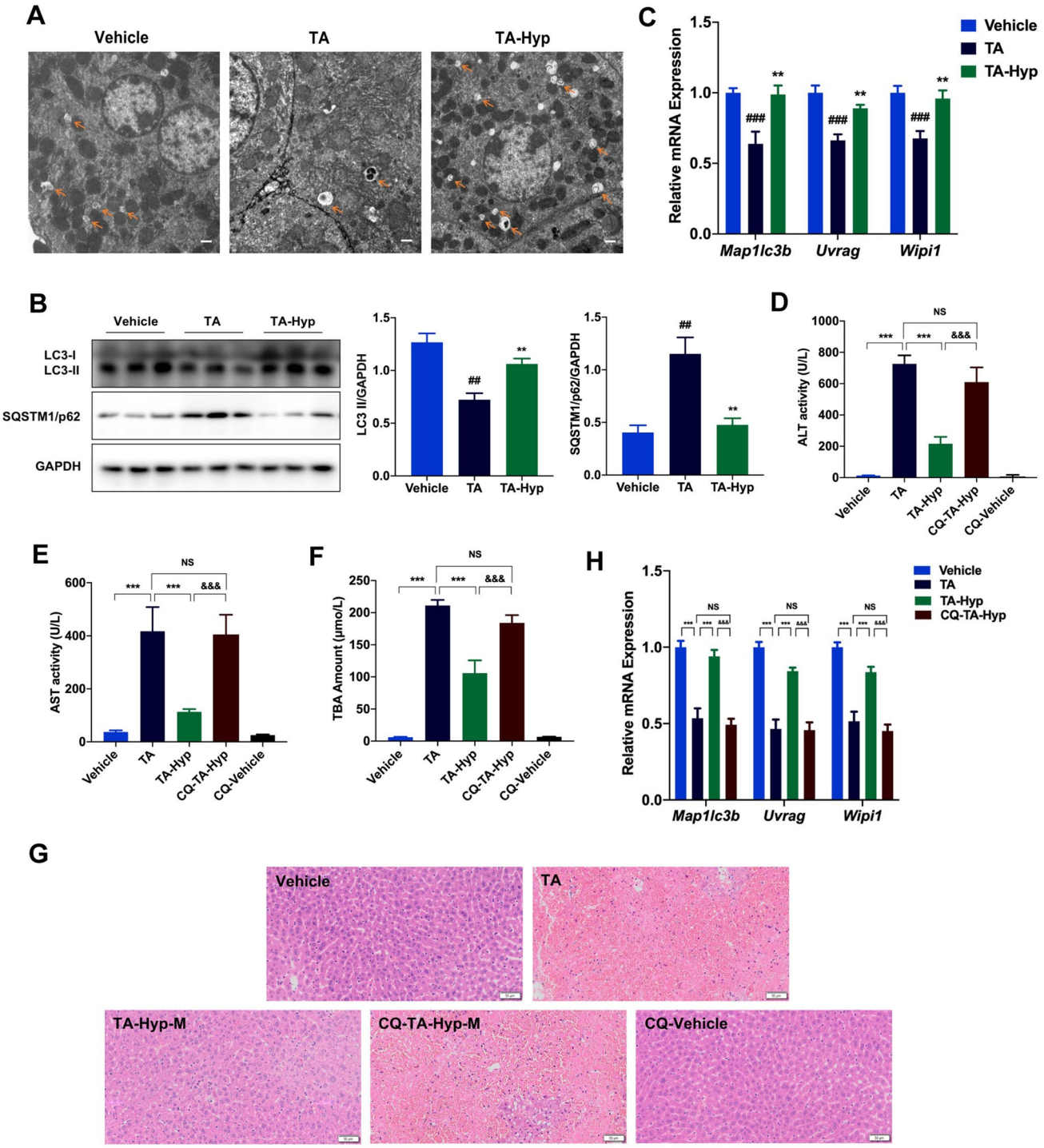

Fig. 3 Hyp attenuates PA-induced liver injury by enhancing autophagy in mice. **A** Representative TEM micrographs of mouse liver autophagic vacuoles from each group. Orange arrows indicate autophagic vacuoles. Scale bars, 10 μm. **B** The expression of the proteins LC3-II and SQSTM1/p62 were measured by western blotting in mouse liver. Bar graphs show summary data (n = 3). **C** The mRNA levels of autophagy-associated genes (*Map1lc3b*, *Uvrag*, *Wipi1*) were evaluated by qRT-PCR (n = 6). **D** The mice were orally administered TA, and then subjected to two administrations of Hyp at 6 h and 30 h post-TA treatment. Chloroquine was intraperitoneally injected into mice once (1 h prior to Hyp administration, at 5 h). Serum ALT activity (n = 6). **E** Serum AST activity (n = 6). **F** Serum TBA amount (n = 6). **G** Representative images of H&E-stained liver sections (scale bars, 50 μm). **H** The mRNA levels of autophagy-associated genes (*Map1lc3b*, *Uvrag*, *Wipi1*) were evaluated by qRT-PCR in chloroquine-treated mice (n = 6). **A–H** Hyp, 40 mg/kg. Data were shown as the means ± SEM and analyzed by one-way ANOVA or Student's *t*-test. **B, C** $^{\#\#}P < 0.01$, $^{\#\#\#}P < 0.001$ vs. Vehicle; $^{**}P < 0.01$ vs. TA. **D–F, H** $^{***}P < 0.001$ vs. TA; $^{\&\&\&}P < 0.001$ vs. TA-Hyp

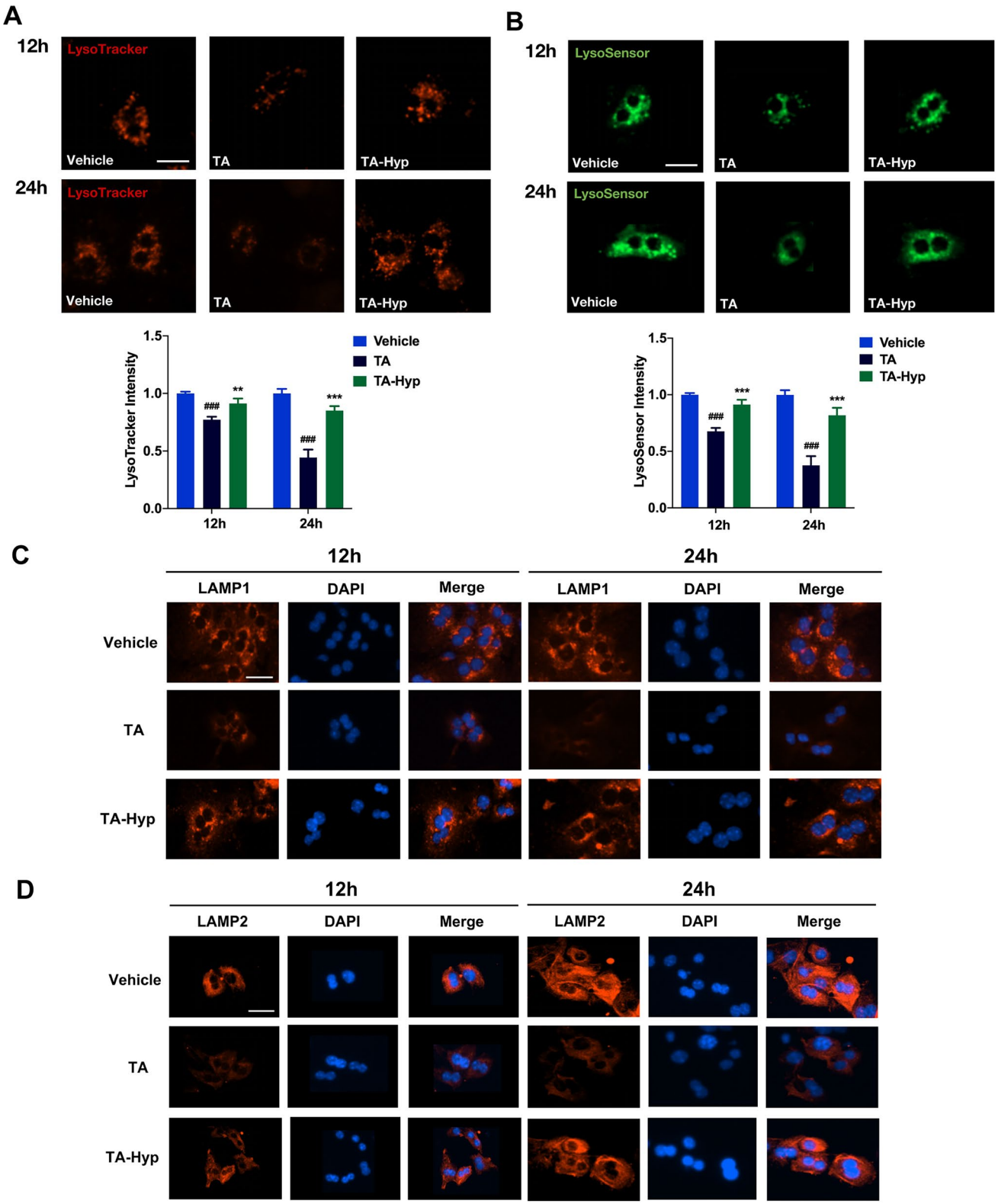

Fig. 4 Hyp attenuates PA-induced impairment of lysosomal function. Primary hepatocytes were treated with TA for 12 h or 24 h. Hyp was added to the cultures 1 h before TA treatment. **A, B** Representative images of LysoTracker Red- and LysoSensor Green-staind in primary hepatocytes. Summary data show LysoTracker Red and LysoSensor Green fluorescent intensities. Scale bars, 200 μm. **C, D** Representative immunofluorescence images of LAMP1 and LAMP2 in primary hepatocytes. Scale bars, 200 μm. **A–D** Hyp, 50 μM. Data were shown as the means ± SD from at least three independent experiments and analyzed by one-way ANOVA. $^{###}P < 0.001$ vs. Vehicle; $^{**}P < 0.01$, $^{***}P < 0.001$ vs. TA

Hyp treatment in a time-dependent manner (Fig. 4A, B). We further validated that Hyp treatment could mitigate TA-induced lysosomal dysfunction via IF analysis using antibodies against lysosomal-associated membrane proteins 1 and 2 (LAMP1 and LAMP2). TA-treated primary hepatocytes showed considerable reductions in LAMP1 and LAMP2 expression (Fig. 4C, D). In addition, WB revealed that TA-treated primary hepatocytes had less LAMP1 protein than vehicle-treated cells (Supplementary Fig. 2A). This result suggested that the lysosome number and integrity were both disrupted by TA treatment and that Hyp reversed these disruptions in a dose- or time-dependent manner. Overall, these findings suggest that Hyp can alleviate the PA-induced impairment of lysosomal function.

Hyp attenuates PA-induced liver injury through TFEB activation

To further corroborate the effect of Hyp on TFEB activation in PA-induced liver injury, subcellular fractionation was used to confirm TFEB localization. As shown in Fig. 5A, WB analysis revealed that the nuclear levels of TFEB were significantly decreased in TA-treated mouse livers compared with vehicle-treated mouse livers. Notably, Hyp treatment efficiently reversed these effects. Moreover, Hyp administration enhanced LAMP1 protein expression in TA-treated mice (Supplementary Fig. 2B). To further confirm TFEB's nuclear localization in mouse hepatocytes, we performed an IF assay, which revealed substantial TFEB localization in response to Hyp in TA-treated mouse liver tissues compared to non-Hyp-treated mouse liver tissues (Fig. 5B). Consistently, Hyp promoted TFEB nuclear localization in TA-stimulated primary hepatocytes (Fig. 5C). Furthermore, the IF results also showed that Hyp treatment increased the ratio of nuclear to cytosolic TFEB levels in primary hepatocytes (Fig. 5D). Taken together, these findings suggest that Hyp may attenuate PA-induced liver injury through TFEB nuclear translocation.

Hyp improves PA-induced mitochondrial dysfunction by activating the TFEB-PGC1α pathway

The expression of PGC1α is directly regulated by TFEB in a key regulatory mechanism in mitochondrial biogenesis (Settembre et al. 2013). Since we found that Hyp promoted TFEB translocation to the nucleus, we investigated whether Hyp could modulate mitochondrial biogenesis by activating the TFEB pathway. To do so, we first examined the impact of Hyp on mitochondrial bioenergetics in primary hepatocytes exposed to TA. The results suggest that Hyp has a beneficial effect in restoring ATP depletion in TA-exposed hepatocytes (Supplementary Fig. 3A). Hyp also prevented TA-induced collapse of the ΔΨm (Supplementary Fig. 3B). MitoTracker staining revealed that Hyp induced an increase in the number of mitochondria in TA-treated hepatocytes (Supplementary Fig. 3C). Moreover, Hyp treatment inhibited the loss of crucial mitochondrial proteins such as cytochrome C (Cyt C) from the mitochondrial space that was induced by TA exposure (Supplementary Fig. 3D). Consistently, TEM revealed an increased in the number of fragmented and swollen mitochondria in TA-treated primary hepatocytes, and this phenomenon was reversed after Hyp treatment (Supplementary Fig. 3E). In addition, Hyp treatment ameliorated TA-induced mitochondrial dysfunction by increasing the expression of PGC1α (Supplementary Fig. 3F). To investigate the mechanistic importance of TFEB in protecting mitochondria from PA-induced mitochondrial dysfunction, we utilized scRNA or siTFEB to downregulate the expression of the TFEB gene. Interestingly, Hyp increased the expression of PGC1α in TA-treated primary hepatocytes. The PGC1α levels in Hyp-treated, siTFEB-transfected and TA-stimulated primary hepatocytes were similar to those in TA-stimulated hepatocytes (Supplementary Fig. 3G). Notably, PGC1α and peroxisome proliferator-activated receptor α (PPARα) interact with each other to activate the production of certain fatty acid-metabolizing enzymes, including carnitine palmitoyltransferase 1 (CPT1), which may lead to an increase in the mitochondrial β-oxidation of fatty acids (Pessayre et al. 2012; Mansouri et al. 2018). IB analysis revealed that Hyp increased the protein expression of CPT1α and PPARα in TA-treated primary hepatocytes (Supplementary Fig. 3H). These data collectively suggest that Hyp can increase mitochondrial biogenesis through activation of TFEB in primary hepatocytes.

We further evaluated the protective effect of Hyp against PA-induced mitochondrial dysfunction in vivo. Consistent with the results in primary hepatocytes, Hyp restored serum ATP levels as well as cytosolic and mitochondrial Cyt C levels in TA-treated mouse livers (Fig. 6A, B). Simultaneously, we found that PGC1α levels were markedly decreased in TA-treated mouse livers compared with vehicle-treated mouse livers but that these reductions were ameliorated by Hyp treatment (Fig. 6C). Additionally, Hyp restored the mRNA expression levels of the genes related to mitochondrial biogenesis that were inhibited by TA (*Pgc1α*, *Nrf1*, *Tfam*) (Fig. 6D). Hyp also rescued the hepatic levels of CPT1α and PPARα in TA-treated mice (Fig. 6E). Consistently, TA decreased the mRNA levels of *Cpt1α* and *Pparα*, which were significantly recovered by Hyp (Fig. 6F). Together, these results demonstrate mechanistically that Hyp can attenuate PA-induced mitochondrial dysfunction through the TFEB-PGC1α pathway.

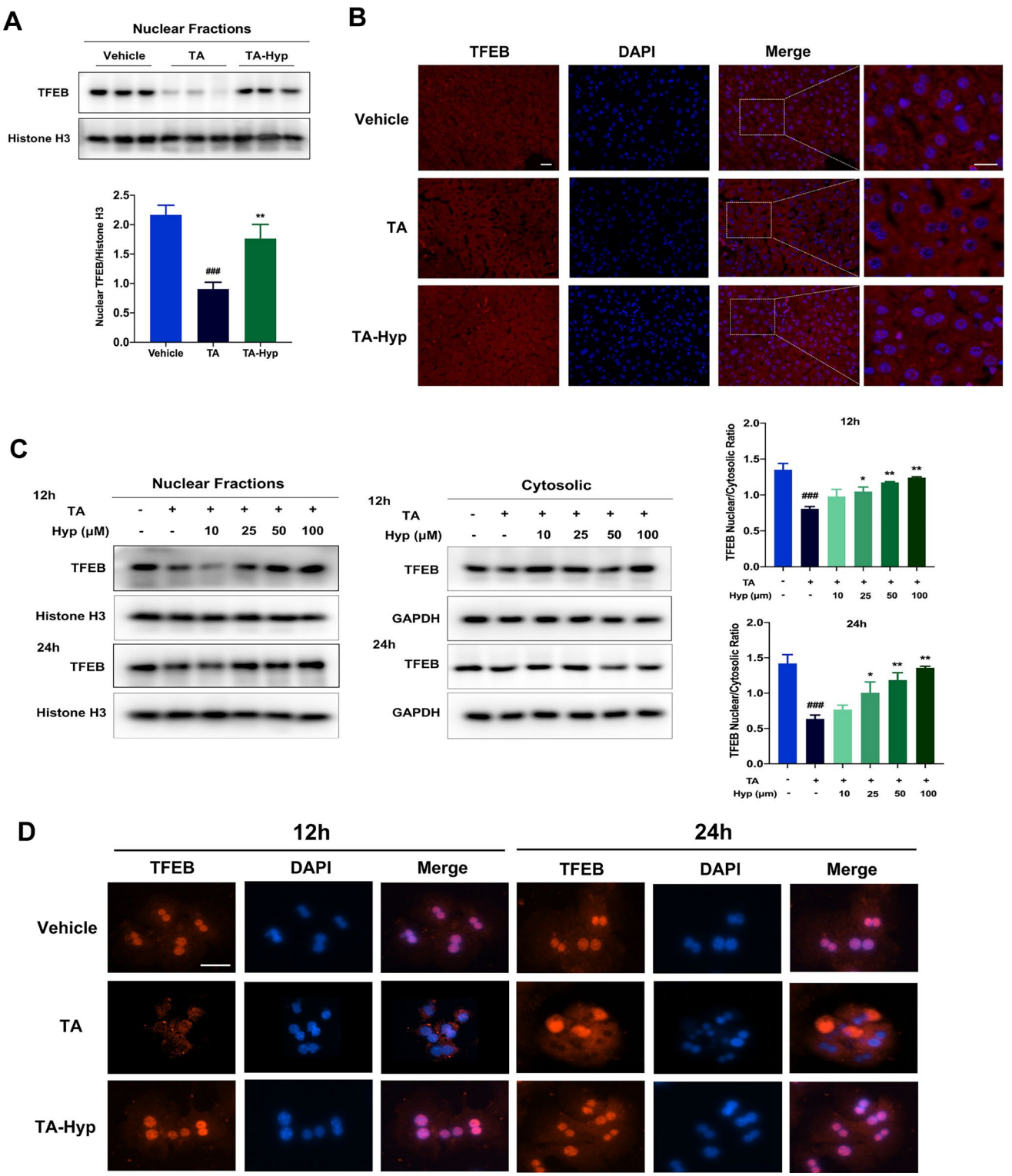

Fig. 5 Hyp attenuates PA-induced liver injury through TFEB activation. **A** Nuclear fractions of TFEB in mouse liver was analyzed by western blotting. Bar graphs show summary data (n = 3). **B** Paraffin sections of mouse liver were stained with TFEB (red) and DAPI (blue). Scale bars, 50 μm (wireframe indicates the magnified image). **C** Nuclear and cytosolic fractions of TFEB in primary hepatocytes were analyzed by western blotting. Bar graphs show summary data. **D** Representative immunofluorescence images of TFEB in primary hepatocytes. Scale bars, 200 μm. **A, B** Hyp, 40 mg/kg. **C, D** Hyp, 50 μM. **A** Data were shown as the means ± SEM and analyzed by one-way ANOVA. **C** Data were shown as the means ± SD from at least three independent experiments and analyzed by one-way ANOVA. $^{###}P < 0.001$ vs. Vehicle; $^{*}P < 0.05$, $^{**}P < 0.01$ vs. TA

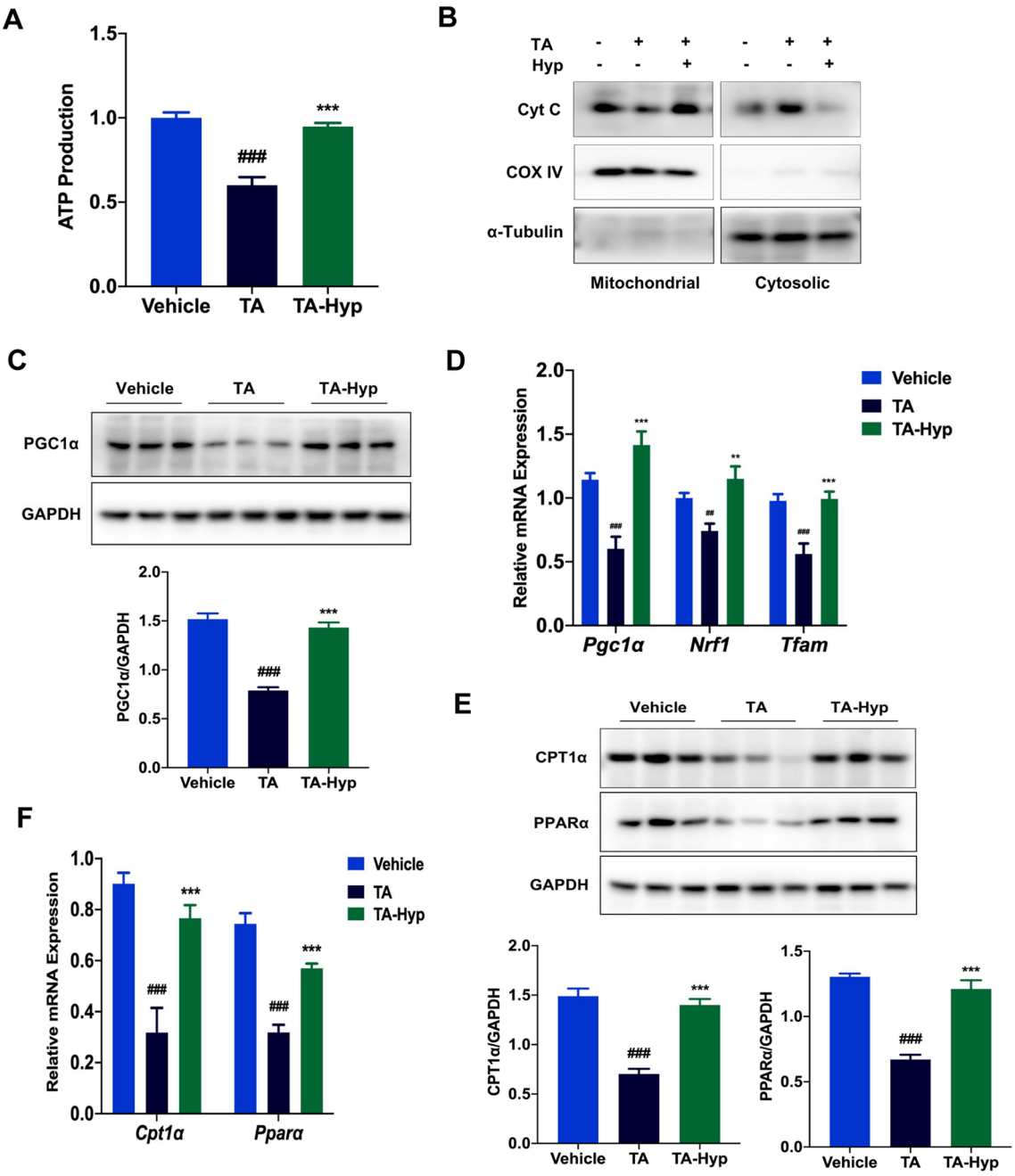

Fig. 6 Hyp induces mitochondrial biogenesis through the TFEB-PGC1α pathway in PAs-treated mouse liver. **A** Serum ATP level (n = 6). **B** Mouse livers were fractionated into mitochondria and cytosol, and the level of Cyt C was analyzed by western blotting. Fraction quality was verified by immunoblotting with markers for the mitochondria (COX IV) and cytoplasm (α-Tubulin) (n = 3). **C** The expression of the protein PGC1α was measured by western blotting in mouse liver. Bar graphs show summary data (n = 3). **D** The mRNA levels of mitochondrial biogenesis-associated genes (*Pgc1α*, *Nrf1*, *Tfam*)) were evaluated by qRT-PCR (n = 6). **E** The expression of the proteins CPT1α and PPARα were measured by western blotting in mouse liver. Bar graphs show summary data (n = 3). **F** The mRNA levels of *Cpt1α* and *Pparα* were evaluated by qRT-PCR (n = 6). **A–F** Hyp, 40 mg/kg. Data were shown as the means ± SEM and analyzed by one-way ANOVA. $^{###}P < 0.001$ vs. Vehicle; $^{**}P < 0.01$, $^{***}P < 0.001$ vs. TA

Inhibition of TFEB expression blocks the beneficial effects of Hyp against PA-induced liver injury

Our investigation further elucidated the significance of the TFEB-mediated autophagy-lysosomal pathway and mitochondrial biogenesis in the beneficial effects of Hyp against PA-induced hepatic injury. Compared with vehicle treatment, Hyp treatment did not prevent PA-induced increases

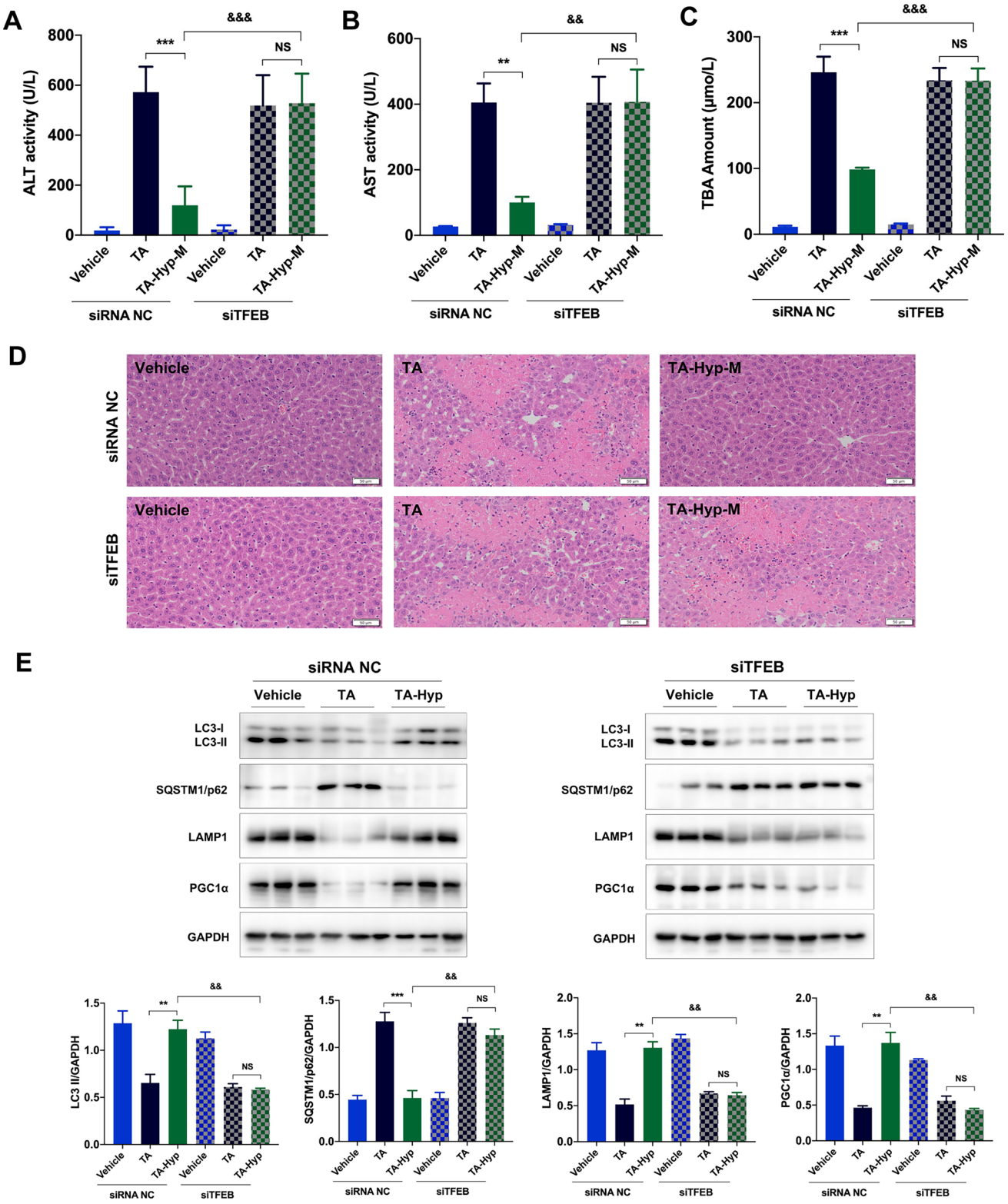

Fig. 7 TFEB mediates the beneficial effects of Hyp in PA-induced liver injury. **A** Serum ALT activity (n = 5). **B** Serum AST activity (n = 5). **C** Serum TBA amount (n = 5). **D** Representative images of H&E-stained liver sections (scale bars, 50 μm). **E** The expression of the proteins LC3-II, SQSTM1/p62, LAMP1, and PGC1α were measured by western blotting in mouse liver. Bar graphs show summary data (n = 3). **A–E** Hyp, 40 mg/kg. Data were shown as the means ± SEM and analyzed by one-way ANOVA or Student's *t*-test. $^{**}P < 0.01$, $^{***}P < 0.001$ vs. TA; $^{\&\&}P < 0.01$, $^{\&\&\&}P < 0.001$ vs. TA-Hyp (siRNA NC)

in the serum levels of ALT, AST, and TBA (Fig. 7A–C), or liver injury (Fig. 7D) in siTFEB-treated mice. Notably, in the siTFEB-treated mice, Hyp did not influence the mRNA levels of the genes associated with autophagy-lysosomal function and mitochondrial biogenesis (Supplementary Fig. 4). Furthermore, siTFEB-treated mice did not display Hyp-induced enhancement of SQSTM1/p62 degradation, LC3-II formation, and LAMP1 and PGC1α protein abundance (Fig. 7E). The results collectively suggest that the induction of the autophagy-lysosomal pathway and mitochondrial biogenesis by TFEB is mainly responsible for the beneficial effects of Hyp in PA-induced liver injury.

Hyp activates TFEB in PA-induced liver injury through inhibition of mTORC1 activity

In our investigation, we first assessed the effect of Hyp on primary hepatocytes, as we have shown its inability to activate TFEB and induce TFEB nuclear translocation (Supplementary Fig. 5). Phosphorylation of TFEB is the primary factor that determines TFEB subcellular localization in liver cells. The two main protein kinases that are known to phosphorylate TFEB and preserve it in an inactive state in the cytosol are mTORC1 and extracellular signal-regulated kinase 2 (ERK2). As depicted in Supplementary Fig. 6A, we found that preincubation of primary hepatocytes with Hyp inhibited TA-induced mTORC1 activation, with little effect on the ERK1/2 signaling pathway. TA also led to increases in the levels of phosphorylated S6 and eIF4E, two well-known substrate proteins that are phosphorylated by mTORC1. These increases were reversed by Hyp treatment in a manner dependent on both dose and time (Supplementary Fig. 6B). Additionally, the nuclear TFEB protein level was increased in the presence of Torin1 (an mTORC1 inhibitor) similar to the effect observed with Hyp treatment (Supplementary Fig. 6C). We further found that the expression of nuclear TFEB was markedly decreased by pretreatment with MHY 1485 (an mTORC1 activator) before Hyp treatment in TA-stimulated primary hepatocytes (Supplementary Fig. 6D).

The basis of Hyp-mediated TFEB nuclear localization was further elucidated through inhibition of mTORC1 activity in vivo. WB revealed that TA significantly increased the levels of phosphorylated mTOR, S6, and eIF4E but that these increases were reversed by Hyp treatment. However, phosphorylated ERK1/2 levels were not altered by TA exposure compared to vehicle treatment (Fig. 8A). Since PAs caused mTORC1 activation, we investigated whether inhibiting mTORC1 could reduce the mTORC1-mediated inactivation of TFEB and the contemporaneous liver injury induced by PAs. We found that Torin1 significantly alleviated PA-induced hepatotoxicity, as demonstrated by serum biochemical analysis and H&E staining (Supplementary Fig. 7A–D). WB indicated that Torin1 caused extensive nuclear accumulation of TFEB (Supplementary Fig. 7E). Moreover, TA inhibited the mRNA expression of multiple TFEB target genes, which was subsequently restored by Torin1 (Supplementary Fig. 7F). Consistent with the WB results, Torin1-treated mouse livers showed increased nuclear distribution of TFEB compared with TA-only-treated mouse livers in IF staining (Supplementary Fig. 7G). In contrast, when we administered MHY 1485 to mice, we found that it abrogated the protective effect of Hyp against PA-induced hepatotoxicity. As illustrated in Fig. 8B–E, MHY 1485 exacerbated the effects of Hyp in decreasing the serum levels of ALT, AST, and TBA, as visualized by H&E staining. MHY 1485 also reversed the Hyp-induced increases in TFEB phosphorylation and the mRNA expression levels of TFEB target genes in PA-induced liver injury (Fig. 8F, G). Furthermore, IF staining of TFEB revealed reduced nuclear accumulation of TFEB in the livers of mice treated with MHY 1485 and Hyp compared with those of mice treated with PAs alone, whereas TFEB staining in the livers of Hyp-treated mice showed the opposite pattern (Supplementary Fig. 8). Collectively, these data suggest that Hyp can improve TFEB nuclear translocation and attenuate PA-induced liver injury through inhibition of mTORC1 activity, whereas activation of mTORC1 can abrogate the protective effect of Hyp in PA-induced hepatotoxicity.

Discussion

In this study, we measured the protective effect of Hyp against PA-induced liver injury. Our study demonstrates that Hyp can ameliorate PA-induced hepatotoxicity through the regulation of mitochondrial homeostasis. Furthermore, we found that, through inhibition of mTORC1 activity, Hyp promotes TFEB nuclear translocation associated with the autophagy-lysosomal pathway and mitochondrial biogenesis.

Mitochondrial dysfunction is increasingly being recognized as a key precipitant of PA-induced hepatic injury (Neuman et al. 2015; Yang et al. 2017; Wang et al. 2020). In this scenario, the mitochondria are significantly altered by functional deficits and structural damage, such as an imbalance in the mitochondrial fission–fusion ratio, overproduction of ROS, and exacerbation of apoptosis (Huang et al. 2019; Wang et al. 2020). Our findings were consistent with those of prior studies, indicating that mitochondrial dysfunction was present in PA-treated mice. Therefore, targeting mitochondrial preservation may be an effective therapeutic approach for the treatment of liver damage caused by PAs.

By examining how PA-induced liver injury was ameliorated by Hyp, we observed upregulation of genes associated with the autophagy-lysosomal pathway in the livers of mice administered Hyp, and we found that this upregulation was

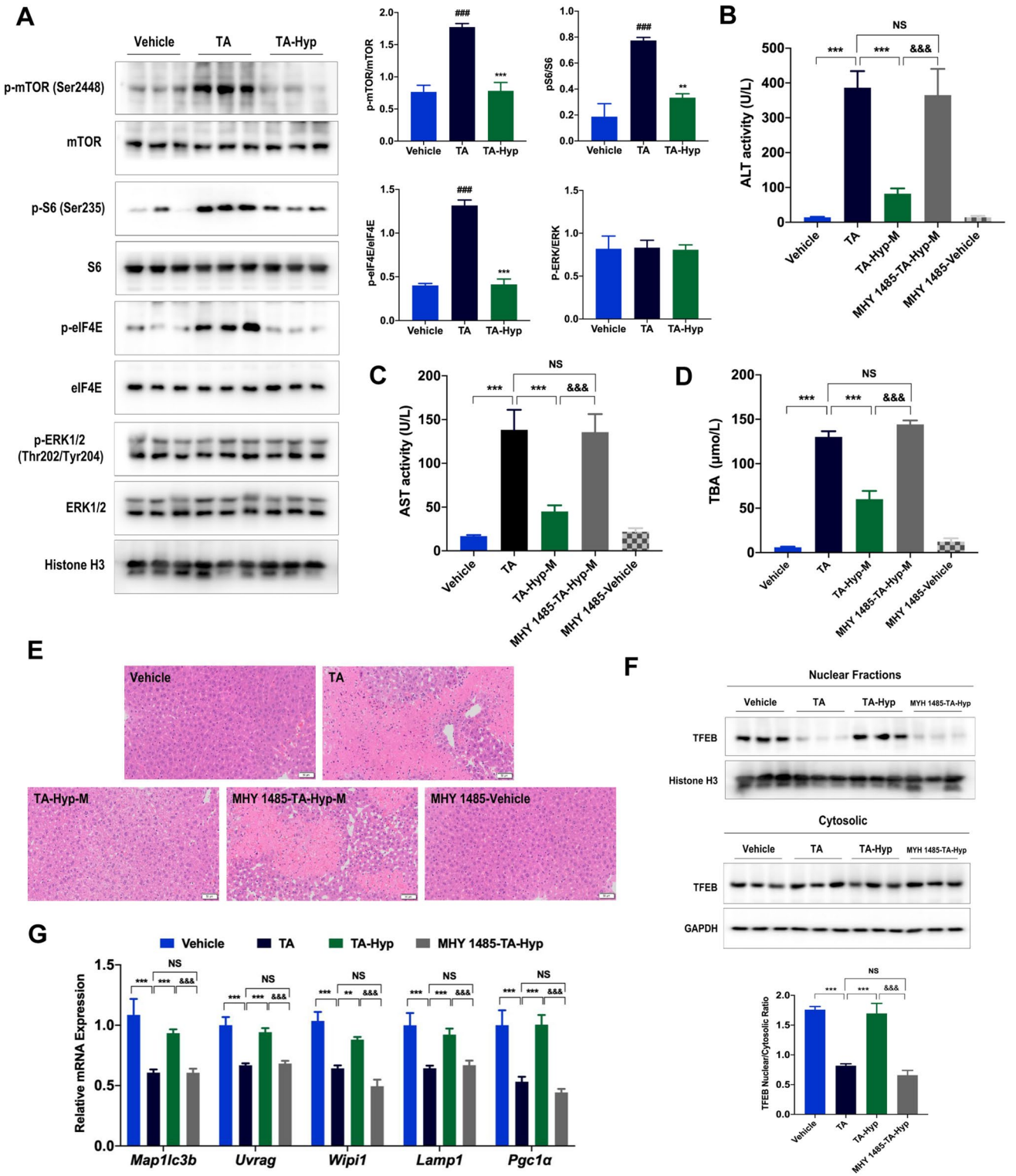

Fig. 8 Inhibition of mTOR1 activity by Hyp attenuates PA-induced liver injury in mice. **A** The expression of the proteins p-mTORC, p-S6, p-eIF4E, and p-ERK1/2 were measured by western blotting in mouse liver. Bar graphs show summary data (n = 3). **B** The mice were orally administered TA and then subjected to two administrations of Hyp at 6 h and 30 h post-TA treatment. MHY 1485 was intraperitoneally injected into mice once (1 h prior to Hyp administration, at 5 h). Serum ALT activity (n = 6). **C** Serum AST activity (n = 6). **D** Serum TBA amount (n = 6). **E** Representative images of H&E-stained liver sections (scale bars, 50 μm). **F** Nuclear and cytosolic fractions of TFEB in mouse liver were analyzed by western blotting. Bar graphs show summary data (n = 3). **G** The mRNA levels of TFEB target genes (*Map1lc3b*, *Uvrag*, *Wipi1*, *Lamp1*, *Pgc1α*) were evaluated by qRT-PCR (n = 6). **A-G** Hyp, 40 mg/kg. Data were shown as the means ± SEM and analyzed by one-way ANOVA or Student's *t*-test. **A** $^{\#\#\#}P < 0.001$ vs. Vehicle; $^{**}P < 0.01$, $^{***}P < 0.001$ vs. TA. **B–D, F, G** $^{**}P < 0.01$, $^{***}P < 0.001$ vs. TA; $^{\&\&\&}P < 0.001$ vs. TA-Hyp

dependent on TFEB activation. In this study, LC3-II flux and SQSTM1/p62 accumulation were used as functional readouts of autophagic activity in affected liver cells (Liu et al. 2016; Mizushima et al. 2010). Our observations revealed a decrease in the level of LC3-II and an increased accumulation of SQSTM1/p62 in PA-induced hepatotoxicity, both of which were attenuated by Hyp. Given that autophagy is a dynamic process, an increase in the LC3-II level can reflect either increased formation of autophagosomes or suppressed clearance of autophagosomes. Thus, a lysosomal inhibitor was applied to evaluate the effect of Hyp on autophagic flux in PA-induced liver injury. Our results suggest that Hyp can alleviate PA-induced liver injury by enhancing autophagic flux. The ultimate step in the autophagy process is the degradation of the cargo in lysosomes. The results indicated that PAs reduced lysosomal abundance and changed the lysosomal pH but that both of these effects were markedly reversed by Hyp. LAMPs are the primary protein components of the lysosomal membrane, and they play a significant role in controlling the structural integrity of lysosomes as well as in the autophagic pathway (Eskelinen 2006; Schwake et al. 2013). Here, we identified decreases in the levels of LAMP1 and LAMP2 in PA-treated primary hepatocytes or mouse livers that were reversed by Hyp treatment. Thus, we inferred that Hyp eliminated the PA-induced reductions in the total lysosome number and the integrity of lysosomes. These experimental results were consistent with previous reports that the activation of TFEB increases liver autophagy-lysosomal function (Settembre et al. 2013; Pastore et al. 2017). Therefore, multiple downstream effectors of the autophagy-lysosomal pathway mediated by TFEB activation might be involved in the process by which Hyp attenuates PA-induced liver injury.

Our study highlights a novel mechanism by which Hyp attenuates PA-induced mitochondrial dysfunction by activating the TFEB-PGC1α pathway. Notably, the expression of TFEB and its subcellular localization are changed in liver injury (Chao et al. 2018, 2021). According to previous studies, TFEB function and stability are regulated mainly by the TFEB phosphorylation status. Phosphorylated TFEB first stays in the cytoplasm but then translocates to the nucleus during the dephosphorylation process (Raben and Puertollano 2016; Puertollano et al. 2018). Our results further revealed that the decrease in TFEB nuclear expression was concomitant with a reduction in TFEB transcriptional activity in PA-treated primary hepatocytes or mouse livers but that both of these effects were significantly attenuated by Hyp. PGC-1α plays an instrumental role as a crucial transcriptional regulator of mitochondrial biogenesis and subsequent mitochondrial fatty acid β-oxidation (Pessayre et al. 2012; Mansouri et al. 2018). Our study revealed that Hyp stimulated mitochondrial biogenesis by inducing mitochondrial turnover through activation of PGC1α, leading to restoration of the population of normally functioning mitochondria. Moreover, Hyp significantly attenuated the decreases in the expression of fatty acid β-oxidation-associated genes after PA treatment. Additionally, the results demonstrated that silencing TFEB abrogated the beneficial effect of Hyp on PA-induced mitochondrial dysfunction, providing further evidence that TFEB mediates the effect of Hyp in promoting mitochondrial biogenesis. Collectively, these findings suggest that Hyp ameliorates mitochondrial dysfunction through activation of the TFEB-PGC1α pathway in PA-induced hepatic injury.

The nuclear translocation of TFEB is regulated by the TFEB phosphorylation status. At least two different kinases have been shown to phosphorylate TFEB, namely, mTORC1 and ERK2 (Settembre et al. 2013). In the current study, we found that PAs increased mTORC1 activation in both primary hepatocytes and mouse livers but that this increase was significantly reversed by Hyp. As previously reported, TFEB is negatively regulated by mTORC1, where mTORC1 inactivates TFEB through phosphorylation; however, mTORC1 inactivation during starvation induces TFEB dephosphorylation and activation (Roczniak-Ferguson et al. 2012; Martina et al. 2012; Martina and Puertollano 2013). We were able to show that inhibition of mTORC1 activity in the presence of PAs led to increases in the nuclear accumulation of TFEB and the expression of its target genes, suggesting that TFEB dysfunction may be caused by mTORC1 activation. Torin1 (an mTORC1 inhibitor) reversed the PA-induced reductions in hepatic TFEB protein levels, further supporting the pivotal role of mTORC1 in regulating PA-induced TFEB inactivation. Furthermore, the mTORC1 activator MHY 1485 partially abrogated the beneficial effect of Hyp in PA-induced hepatotoxicity, while MHY 1485 downregulated hepatic TFEB protein, indicating the crucial role of mTORC1 in Hyp-mediated hepatoprotection. We deduced that ERK1/2 may not play a critical role in PA-induced TFEB inactivation given that PAs did not activate ERK1/2 and that ERK1/2 signaling remained unchanged even after Hyp treatment.

PAs are some of the most hepatotoxic natural compounds and are ubiquitously distributed worldwide. Liver metabolism and the molecular hepatotoxicity mechanisms of PAs include various processes, especially oxidative stress, apoptosis, and (dysregulated) metabolism of bile acids. Our study highlights that Hyp can activate the TFEB-mediated autophagy-lysosomal pathway and mitochondrial biogenesis by inhibiting mTORC1 activity, thereby alleviating the mouse liver injury induced by PAs. Notably, overdose of APAP is a leading contributor to drug-induced acute liver failure in many developed countries. Thus far, several mechanisms have been found to be involved in the pathogenesis of APAP-induced acute liver injury, such as phase I metabolism, phase II metabolism, oxidative stress,

endoplasmic reticulum stress, autophagy, sterile inflammation, and microcirculatory dysfunction (Yan et al. 2018). According to prior research, Hyp protects the liver against APAP-induced damage primarily by accelerating the harmless metabolism of APAP (Xie et al. 2016) and by preventing oxidative stress-induced liver injury caused by APAP (Hu et al. 2020). Thus, these findings suggest a different mechanism of action underlying the role of Hyp in treating PA-induced hepatotoxicity compared to that underlying APAP-induced acute liver injury.

In conclusion, the present study demonstrates that Hyp can activate the TFEB-mediated autophagy-lysosomal pathway and mitochondrial biogenesis through inhibition of mTORC1 activity in PA-induced liver injury. These findings provide a novel mechanism supporting Hyp as a potential therapeutic for PA-induced liver injury management.

Supplementary Information The online version contains supplementary material available at https://doi.org/10.1007/s12272-023-01460-3.

Acknowledgements This work is financially supported by the National Natural Science Foundation of China (No. 81920108033; 82074011; 82130115) and the Program of Shanghai Municipal Health Commission (No. ZY (2021–2023)-0215).

Data availability The data that support the findings of this study are not openly available due to resasons of sensitivity and are available from the corresponding author upon reasonable request.

Declarations

Conflict of interest The authors declare that they have no known competing financial interests or personal relationships that could have appeared to influence the work reported in this paper.

References

Chalasani NP, Maddur H, Russo MW, Wong RJ, Reddy RK (2021) ACG clinical guideline: the diagnosis and management of idiosyncratic drug-induced liver injury. Am J Gastroenterol 116:878–898. http://dio.org/10.14309/ajg.0000000000001259

Chao X, Wang S, Zhao K, Li Y, Williams JA, Li T, Chavan H, Krishnamurthy P, He XC, Li L, Ballabio A, Ni HM, Ding W (2018) Impaired TFEB-mediated lysosome biogenesis and autophagy promote chronic ethanol-induced liver injury and steatosis in mice. Gastroenterology 155:865–879. https://doi.org/10.1053/j.gastro.2018.05.027

Chao X, Wang S, Yang L, Ni HM, Ding W (2021) Trehalose activates hepatic transcription factor EB (TFEB) but fails to ameliorate alcohol-impaired TFEB and liver injury in mice. Alcohol Clin Exp Res 45:1950–1964. https://doi.org/10.1111/acer.14695

Eskelinen EL (2006) Roles of LAMP-1 and LAMP-2 in lysosome biogenesis and autophagy. Mol Aspects Med 27:495–502. https://doi.org/10.1016/j.mam.2006.08.005

Han D, Dara L, Win S, Than TA, Yuan L, Abbasi SQ, Liu ZX, Kaplowitz N (2013) Regulation of drug-induced liver injury by signal transduction pathways: critical role of mitochondria. Trends Pharmacol Sci 34:243–253. https://doi.org/10.1016/j.tips.2013.01.009

Hu C, Chen Y, Cao Y, Jia Y, Zhang J (2020) Metabolomics analysis reveals the protective effect of quercetin-3-O-galactoside (Hyperoside) on liver injury in mice induced by acetaminophen. J Food Biochem 3:e13420. https://doi.org/10.1111/jfbc.13420

Huang Z, Jing X, Sheng Y, Zhang J, Hao Z, Wang Z, Ji L (2019) (-)-Epicatechin attenuates hepatic sinusoidal obstruction syndrome by inhibiting liver oxidative and inflammatory injury. Redox Biol 22:101117. https://doi.org/10.1016/j.redox.2019.101117

Hunt CM (2010) Mitochondrial and immunoallergic injury increase risk of positive drug rechallenge after drug-induced liver injury: a systematic review. Hepatology 52:2216–2222. https://doi.org/10.1002/hep.24022

Kaplowitz N (2005) Idiosyncratic drug hepatotoxicity. Nat Rev Drug Discov 4:489–499. https://doi.org/10.1038/nrd1750

Leise MD, Poterucha JJ, Talwalkar JA (2014) Drug-induced liver injury. Mayo Clin Proc 89:95–106. https://doi.org/10.1016/j.mayocp.2013.09.016

Liesa M, Palacin M, Zorzano A (2009) Mitochondrial dynamics in mammalian health and disease. Physiol Rev 89:799–845. https://doi.org/10.1152/physrev.00030.2008

Liu W, Ye L, Huang W, Guo L, Xu Z, Wu H, Yang C, Liu H (2016) p62 links the autophagy pathway and the ubiquitin-proteasome system upon ubiquitinated protein degradation. Cell Mol Biol Lett 21:29. https://doi.org/10.1186/s11658-016-0031-z

Lu Y, Ma J, Song Z, Ye Y, Fu PP, Lin G (2018) The role of formation of pyrrole-ATP synthase subunit beta adduct in pyrrolizidine alkaloid-induced hepatotoxicity. Arch Toxicol 92:3403–3414. https://doi.org/10.1007/s00204-018-2309-6

Ma X, Liu H, Murphy JT, Foyil SR, Godar RJ, Abuirqeba H, Weinheimer CJ, Barger PM, Diwan A (2015) Regulation of the transcription factor EB-PGC1alpha axis by beclin-1 controls mitochondrial quality and cardiomyocyte death under stress. Mol Cell Biol 35:956–976. https://doi.org/10.1128/MCB.01091-14

Mansouri A, Gattolliat CH, Asselah T (2018) Mitochondrial dysfunction and signaling in chronic liver diseases. Gastroenterology 155:629–647. https://doi.org/10.1053/j.gastro.2018.06.083

Martina JA, Puertollano R (2013) Rag GTPases mediate amino acid-dependent recruitment of TFEB and MITF to lysosomes. J Cell Biol 200:475–491. https://doi.org/10.1083/jcb.201209135

Martina JA, Chen Y, Gucek M, Puertollano R (2012) MTORC1 functions as a transcriptional regulator of autophagy by preventing nuclear transport of TFEB. Autophagy 8:903–914. https://doi.org/10.4161/auto.19653

Middleton E, Kandaswami C, Theoharides TC (2000) The effects of plant flavonoids on mammalian cells: implications for inflammation, heart disease, and cancer. Pharmacol Rev 52:673–751

Mizushima N, Komatsu M (2011) Autophagy: renovation of cells and tissues. Cell 147:728–741. https://doi.org/10.1016/j.cell.2011.10.026

Mizushima N, Yoshimori T, Levine B (2010) Methods in mammalian autophagy research. Cell 140:313–326. https://doi.org/10.1016/j.cell.2010.01.028

Murphy MP (2009) How mitochondria produce reactive oxygen species. Biochem J 417:1–13. https://doi.org/10.1042/BJ20081386

Nakatogawa H, Suzuki K, Kamada Y, Ohsumi Y (2009) Dynamics and diversity in autophagy mechanisms: lessons from yeast. Nat Rev Mol Cell Biol 10:458–467. https://doi.org/10.1038/nrm2708

Navarro VJ, Senior JR (2006) Drug-related hepatotoxicity. N Engl J Med 354:731–739. https://doi.org/10.1056/NEJMra052270

Neuman MG, Cohen L, Opris M, Nanau RM, Hyunjin J (2015) Hepatotoxicity of pyrrolizidine alkaloids. J Pharm Pharm Sci 18:825–843. https://doi.org/10.18433/j3bg7j

Niu C, Ma M, Han X, Wang Z, Li H (2017) Hyperin protects against cisplatin-induced liver injury in mice. Acta Cir Bras 32:633–640. https://doi.org/10.1590/s0102-865020170080000005

Pastore N, Vainshtein A, Klisch TJ, Armani A, Huynh T, Herz NJ, Polishchuk EV, Sandri M, Ballabio A (2017) TFE3 regulates

whole-body energy metabolism in cooperation with TFEB. EMBO Mol Med 9:605–621. https://doi.org/10.15252/emmm.201607204

Pessayre D, Fromenty B, Berson A, Robin MA, Lettéron P, Moreau R, Mansouri A (2012) Central role of mitochondria in drug-induced liver injury. Drug Metab Rev 44:34–87. https://doi.org/10.3109/03602532.2011.604086

Puertollano R, Ferguson SM, Brugarolas J, Ballabio A (2018) The complex relationship between TFEB transcription factor phosphorylation and subcellular localization. EMBO J 37:e98804. https://doi.org/10.15252/embj.201798804

Qian H, Chao X, Williams J, Fulte S, Li T, Yang L, Ding W (2021) Autophagy in liver diseases: a review. Mol Aspects Med 82:100973. https://doi.org/10.1016/j.mam.2021.100973

Raben N, Puertollano R (2016) TFEB and TFE3: linking lysosomes to cellular adaptation to stress. Annu Rev Cell Dev Biol 32:255–278. https://doi.org/10.1146/annurev-cellbio-111315-125407

Raza A, Xu X, Sun H, Tang J, Ouyang Z (2017) Pharmacological activities and pharmacokinetic study of hyperoside: a short review. Trop J Pharma Res 16:483–489. https://doi.org/10.4314/tjpr.v16i2.30

Roczniak-Ferguson A, Petit CS, Froehlich F, Qian S, Ky J, Angarola B, Walther TC, Ferguson SM (2012) The transcription factor TFEB links mTORC1 signaling to transcriptional control of lysosome homeostasis. Sci Signal 5:ra42. https://doi.org/10.1126/scisignal.2002790

Ruivo R, Anne C, Sagne C, Gasnier B (2009) Molecular and cellular basis of lysosomal transmembrane protein dysfunction. Biochim Biophys Acta 1793:636–649. https://doi.org/10.1016/j.bbamcr.2008.12.008

Sardiello M, Palmieri M, di Ronza A, Medina DL, Valenza M, Gennarino VA, di Malta C, Donaudy F, Embrione V, Polishchuk RS, Banfi S, Parenti G, Cattaneo E, Ballabio A (2009) A gene network regulating lysosomal biogenesis and function. Science 325:473–477. https://doi.org/10.1126/science.1174447

Schwake M, Schroder B, Saftig P (2013) Lysosomal membrane proteins and their central role in physiology. Traffic 14:739–748. https://doi.org/10.1111/tra.12056

Settembre C, Malta CD, Polito VA, Arencibia MG, Vetrini F, Erdin S, Erdin SU, Huynh T, Medina D, Colella P, Sardiello M, Rubinsztein DC, Ballabio A (2011) TFEB links autophagy to lysosomal biogenesis. Science 332:1429–1433. https://doi.org/10.1126/science.1204592

Settembre C, Cegli RD, Mansueto G, Saha PK, Vetrini F, Visvikis O, Huynh T, Carissimo A, Palmer D, Klisch TJ, Wollenberg AC, Bernardo DD, Chan L, Irazoqui JE, Ballabio A (2013) TFEB controls cellular lipid metabolism through a starvation-induced autoregulatory loop. Nat Cell Biol 15:647–658. https://doi.org/10.1038/ncb2718

Settembre C, Fraldi A, Medina DL, Ballabio A (2013) Signals from the lysosome: a control centre for cellular clearance and energy metabolism. Nat Rev Mol Cell Biol 14:283–296. https://doi.org/10.1038/nrm3565

Shen T, Liu Y, Shang J, Xie Q, Li J, Yan M, Xu J, Niu J, Liu J, Watkins PB, Aithal GP, Andrade RJ, Dou X, Yao L, Lv F, Wang Q, Li Y, Zhou X, Zhang Y, Zong P, Wan B, Zou Z, Yang D, Nie Y, Li D, Wang Y, Han X, Zhuang H, Mao Y, Chen C (2019) Incidence and etiology of drug-induced liver injury in mainland China. Gastroenterology 156:2230–2241. https://doi.org/10.1053/j.gastro.2019.02.002

Stegelmeier BL, Edgar JA, Colegate SM, Gardner DR, Schoch TK, Coulombe RA, Molyneux RJ (1999) Pyrrolizidine alkaloids plants, metabolism and toxicity. J Nat Toxins 8:95–116

Wang J, Gao H (2014) Tusanqi and hepatic sinusoidal obstruction syndrome. J Dig Dis 15:105–107. https://doi.org/10.1111/1751-2980.12112

Wang Y, Qiao D, Li Y, Xu F (2018) Risk factors for hepatic veno-occlusive disease caused by *Gynura segetum*: a retrospective study. BMC Gastroenterol 18:156. https://doi.org/10.1186/s12876-018-0879-7

Wang W, Yang X, Chen Y, Ye X, Jiang K, Xiong A, Yang L, Wang Z (2020) Seneciphylline, a main pyrrolizidine alkaloid in *Gynura japonica*, induces hepatotoxicity in mice and primary hepatocytes via activating mitochondria-mediated apoptosis. J Appl Toxicol 40:1534–1544. https://doi.org/10.1002/jat.4004

Xie W, Jiang Z, Wang J, Zhang X, Melzig MF (2016) Protective effect of hyperoside against acetaminophen (APAP) induced liver injury through enhancement of APAP clearance. Chem Biol Interact 246:11–19. https://doi.org/10.1016/j.cbi.2016.01.004

Xing H, Fu R, Cheng C, Cai Y, Wang X, Deng D, Gong X, Chen J (2020) Hyperoside protected against oxidative stress-induced liver injury via the PHLPP2-AKT-GSK-3β signaling pathway in vivo and in vitro. Front Pharmacol 11:1065–1077. https://doi.org/10.3389/fphar.2020.01065

Xiong A, Shao Y, Fang L, Yang X, Zhang S, Zheng J, Ding W, Yang L, Wang Z (2019) Comparative analysis of toxic components in different medicinal parts of *Gynura japonica* and its toxicity assessment on mice. Phytomedicine 54:77–88. https://doi.org/10.1016/j.phymed.2018.06.015

Yan M, Huo Y, Yin S, Hu H (2018) Mechanisms of acetaminophen-induced liver injury and its implications for therapeutic interventions. Redox Biol 17:274–283. https://doi.org/10.1016/j.redox.2018.04.019

Yang X, Wang H, Ni HM, Xiong A, Wang Z, Sesaki H, Ding W, Yang L (2017) Inhibition of Drp1 protects against senecionine-induced mitochondria-mediated apoptosis in primary hepatocytes and in mice. Redox Biol 12:264–273. https://doi.org/10.1016/j.redox.2017.02.020

Zheng P, Xu Y, Ren Z, Wang Z, Wang S, Xiong J, Zhang H, Jiang H (2021) Toxic prediction of pyrrolizidine alkaloids and structure-dependent induction of apoptosis in HepaRG cells. Oxid Med Cell Longev 2021:1–12. https://doi.org/10.1155/2021/8822304

Zhu X, Ji M, Han Y, Guo Y, Zhu W, Gao F, Yang X, Zhang C (2017) PGRMC1-dependent autophagy by hyperoside induces apoptosis and sensitizes ovarian cancer cells to cisplatin treatment. Int J Oncol 50:835–846. https://doi.org/10.3892/ijo.2017.3873